573

Absorbing boundary condition for floating two-dimensional objects in current and waves

L.M. SIEREVOGEL and A.J. HERMANS
Department of Technical Mathematics and Informatics
Delft University of Technology
Delft, The Netherlands

Abstract. In this paper an absorbing boundary condition for floating two-dimensional objects in current and waves is studied. A numerical algorithm has been developed, which computes the velocity potential in the physical time domain, by using an artificial boundary to split the infinite fluid domain into a computational part and a residual part. A special Green's function has been developed in the residual part. The condition on the artificial boundary is independent of wave frequency, hence not restricted to harmonic waves. Because of the smaller computational domain and the independence of frequency, the time to compute the hydrodynamic coefficients of floating objects decreases.

Key words: absorbing boundary condition, ship hydrodynamics, domain decomposition, panel method

Introduction

Computing the interaction between waves and the velocity of a ship can be done by using the frequency domain or the physical time domain. The disadvantage of the studies in the frequency domain is their restriction to harmonic waves. Real waves, especially those close to the floating object, are not harmonic. In the time domain we can also handle non-harmonic waves. Several time-domain methods have been developed, most of them are being confined to problems with bodies that have no mean forward speed (for instance Yeung [1], Newman [2] and others). Nakos [3] and Prins and Hermans [4, 5] have developed a two- and three-dimensional time-domain algorithm to compute the behaviour of floating objects in current and waves. In this paper we use the method developed by Prins, because the results are very satisfactory.

The physical fluid domain is infinite (or large). The computational domain cannot be infinite, so we have to introduce artificial boundaries and proper boundary conditions. In the literature, several methods have been proposed to absorb free-surface waves. Romate [6] reviews most of these methods and gives the basic techniques and references. A survey of these methods is given in section 2 . On the basis of Romate's literature survey, Prins decided to use an extension of the Sommerfeld radiation condition for two families of waves. The disadvantage of this Sommerfeld condition is that it is dependent on wave frequency, so it cannot handle non-harmonic waves. Keller and Givoli [7, 8] introduce a method which uses an artificial boundary, dividing the original domain into a computational domain and a residual domain (the interior and the exterior).

In this paper we derive a two-dimensional boundary condition independent of wave frequency, using the idea of Givoli's method with Prins's algorithm. We develop a special Green's function in the exterior. The condition absorbs the outgoing waves. This method also reduces

computer time, when computing the behaviour of an object in harmonic waves. Firstly, the boundary is closer to the object and, secondly, it is not necessary to implement the conditions dependent on every frequency. The two-dimensional results inspired us to tackle the three-dimensional problem as well.

In this paper, we first describe the mathematical model and the numerical algorithm of the time-domain algorithm in the interior. In the second section we give a survey of absorbing boundary conditions and explain our method. Then we present the mathematical model and the numerical algorithm of the exterior. In the fourth section we handle the total problem, the combination of the interior and the exterior. In the results, we first look at the reflections and then we compute the hydrodynamic coefficients, like added mass, damping, movement and the second-order forces.

1. The time-domain algorithm, the interior problem

1.1. MATHEMATICAL MODEL

We reduce the problem of a horizontal circular cylinder with radius R and of infinite length to a two-dimensional one. The cylinder is floating in water of depth h. A uniform current with velocity U and regular incoming waves are travelling in the positive x-direction. The cylinder is free to oscillate in the x- and z-directions, and is free to roll. The coordinate system is chosen such that the undisturbed free surface coincides with the line $z = 0$ and the centre of the circle is located at $x = 0$, $z = 0$.

We assume the following restrictions: there is no viscosity, the fluid is incompressible and homogeneous, and the flow is irrotational. We introduce the velocity potential Φ, which has to satisfy the Laplace equation

$$\nabla^2 \Phi = 0. \tag{1}$$

By using the dynamic and kinematic conditions and splitting the potential into a steady and an unsteady part, like

$$\Phi(x, t) = \overline{\phi}(x) + \phi(x, t) ,$$

we get the linearized free-surface condition

$$\phi_{tt} + g\phi_z + 2\overline{\phi}_x\phi_{xt} + 3\overline{\phi}_x\overline{\phi}_{xx}\phi_x + \overline{\phi}_x^2\phi_{xx} + \overline{\phi}_{xx}\phi_t$$
$$-\frac{1}{2}\left(U^2 - \overline{\phi}_x^2\right)\left(\phi_{xx} - \frac{\phi_{ztt}}{g}\right) = 0 \qquad \text{at } z = 0 , \tag{2}$$

with subscripts denoting the partial derivative and g the gravitational acceleration. The steady potential is represented by the double body potential. For a circle this can be written as

$$\overline{\phi} = Ux + \overline{\phi}_{dist} = Ux\left(1 + \frac{R^2}{x^2 + z^2}\right) . \tag{3}$$

We also use a linearized formulation of the body boundary condition (see Timman and Newman [9])

$$\frac{\partial \phi_{\mathcal{H}}}{\partial n} = \frac{\partial X}{\partial t} \cdot n - X \cdot (n \cdot \nabla)\nabla\overline{\phi}_{\mathcal{H}} ,$$

with $\phi_{\mathcal{H}}$ the potential on the hull and X the displacement of the cylinder.

The bottom is a rigid wall, so we submit the potential on the bottom, ϕ_b, to the condition

$$\frac{\partial \phi_b}{\partial n} = 0 \ . \tag{4}$$

The computational fluid domain is enclosed by a left and a right artificial boundary $\mathcal{B}$. So far we can only say about the potential on this artificial boundary that it satisfies the Laplace equation and that it remains finite if we take $\mathcal{B}$ at infinity (see Fig. 1).

In the following section we give a survey of absorbing boundary conditions. On the basis of the results of the DtN method, we then decide to divide the infinite fluid domain into an interior part and an exterior part. Thus, on both sides of the interior is an exterior $\mathcal{D}$. In the interior S we use the mathematical model described above, which is the same as Prins and Hermans [4] use, but we do not implement a Sommerfeld radiation condition at $\mathcal{B}$.
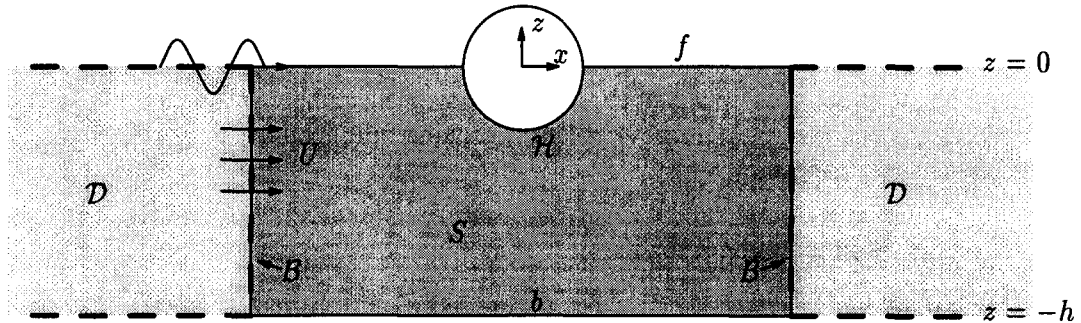

Figure 1. The geometry

1.2. NUMERICAL ALGORITHM

To solve the interior problem, we introduce a Green's function, G, satisfying Eqs. (1) and (4)

$$G(x,\xi) = \frac{1}{2\pi} \log r + \frac{1}{2\pi} \log r_2 \ ,$$

where $r = |x - \xi|$ and $r_2 = |x - \xi'|$, with ξ' the image of ξ with respect to the bottom. By using Green's second theorem, we get for the potential in the interior fluid domain

$$\delta\phi(x,t) = \int_{\partial S \backslash \partial S_b} \left(\phi(\xi,t) \frac{\partial G}{\partial n_\xi}(x,\xi) - G(x,\xi) \frac{\partial \phi}{\partial n_\xi}(\xi,t) \right) \mathrm{d}\Gamma \ ,$$

with

$$\delta = \begin{cases} 1 & x \in S \\ \frac{1}{2} & x \in \partial S \\ 0 & \text{elsewhere} \end{cases} \ ,$$

where ∂S represents the boundary of the domain and ∂S_b the bottom. Green's theorem makes it possible to rewrite the interior problem as follows

$$D\psi(t) = E\psi_n(t) ,$$

with ψ a vector $(\phi_f|\phi_{\mathcal{H}}|\phi_B)$, containing the potential on the free surface, on the hull and on the artificial boundary. To solve this integral equation we discretize the boundaries by dividing these into panels. We assume that the potential has a constant value on such a panel. Prins's approach consists of two steps leading to a Fredholm integral equation of the second kind. Firstly, the free-surface condition (2) and the second-order Sommerfeld radiation condition are discretized with respect to t, where an implicit scheme is used for the time derivation. Secondly, ϕ_n is expressed in ϕ and its tangential derivative along the boundaries, while at the object ϕ_n is supposed to be known. Discretization of the integral equation leads to a matrix equation for the unknown vector ψ

$$D_1\psi_{i+1} = D_2\psi_i + D_3\psi_{i-1} + f_{i+1} , \tag{5}$$

with subscripts denoting the time level and f a time-dependent vector. In our approach we make use of the same algorithm as developed by Prins, except for the boundary B. Experience has taught that the implementation of the Sommerfeld condition on the outer boundary B is efficient if B is taken at a distance of about three wavelengths, while the coefficients for the two families of waves are dependent on the frequency. Hence, the matrix has to be updated for each frequency. Our purpose is to obtain a genuine time method, where the matrix is independent of the frequency.

2. Absorbing boundary conditions

In the literature, several methods have been proposed to absorb free surface waves. These are reviewed in, for instance, Romate [6]. A short description of these methods and some references are given in this section. The most frequently used techniques are:

— **Artificial damping (sponge layer)**

A possibility to absorb the outgoing waves is the use of artificial damping, in particular in the form of a sponge layer. In this method an artificial dissipative term is added to the equations near the artificial boundaries of the truncated domain, so that outgoing waves are absorbed with as little wave reflection as possible. This method is used by, for instance, Israeli and Orszag [10]. The advantage of this method is that it is easy to implement and that it has good reflection properties for a wide range of frequencies, but the disadvantage is that a large domain is needed for the damping zone.

— **Partial differential equations**

Sommerfeld's radiation condition [11] is required to make the problem well posed at infinity and the condition corresponds to the outgoing waves only. For harmonic solutions with wave number k it reads
$$\sqrt{kr}\,(\phi_r - ik\phi) \to 0 \qquad \text{as} \qquad r \to \infty ,$$
or in the time domain
$$c\phi_r - \phi_t \to 0 \qquad \text{as} \qquad r \to \infty ,$$
with c the local phase velocity of the wave to be absorbed. Applying this condition at the artificial boundary gives a set of partial differential equations. Using partial differential equations as an absorbing boundary condition can be done in somewhat different

approaches. The technique which is probably the most widely used was published by Orlanski [12]. He used a first-order equation. The novelty in his approach was that the phase velocity needed in this condition was evaluated numerically in the vicinity of the boundary.

For the acoustic wave problem Engquist and Majda [13] derived a higher-order differential operator at the outer boundary (see also Jones and Kriegsmann [14]). Prins and Hermans [4] use an extension of the Sommerfeld radiation condition for the two wave families, a second-order partial differential equation, which can be written after substituting the phase velocity as

$$\frac{\partial^2 \phi}{\partial t^2} + U \left(\frac{1}{\tau} \pm 2 \right) \frac{\partial^2 \phi}{\partial n \partial t} + U^2 \frac{\partial^2 \phi}{\partial n^2} = 0 \,,$$

with $\tau = (U\omega/g) < 0.25$. This condition is easy to implement, but it absorbs only the waves of which the wave velocity is included. Other waves are partly reflected. Therefore this condition is dependent of the wave frequency.

— Use of exterior solutions
Another way of modelling the absorption of the waves at an artificial boundary is the use of simple exterior solutions. In the exterior, boundaries and boundary conditions are simplified such that an analytical solution can be found. This technique of matching analytical far-field solutions and numerical solutions was, among others, applied by Bai and Yeung [15] to the linearized sea-keeping problem in the frequency domain.

In [16], Yeung gave a time-domain solution of a swaying axisymmetric structure with no mean forward speed. This formulation uses a 'simple-source' representation for the inner domain, while the time-dependent Green's function (used by Newman [2], for instance) is used in the exterior. In principle, this method can be extended to the situation with $U \neq 0$. However, we decided to use a formulation for the discretized free-surface condition.

— DtN relation [1]
For the acoustic-wave equation, Givoli [8] derived a DtN relation at the outer boundary used in combination with a finite-element approach in the interior. This method is very efficient. In the method, a DtN relation is derived, in principle with the help of an explicit solution, by means of the expansion of orthogonal functions. In the frequency domain, the DtN relation becomes homogeneous, while in the time domain an inhomogeneous term originates from the fact that the complete propagating exterior solution has to be taken into account. In the shallow-water case, an orthogonal set of eigenfunctions is available in the exterior. A direct application, however, is much less efficient than in the acoustic case. Too many terms have to be taken into account due to slow convergence. The main result of Givoli is that the complete exterior field has to be taken into account.

We follow the idea of the DtN relation. Because ϕ_n is not expressed in ϕ at the boundaries B in our interior case, our vector of unknowns in Eq.(5) becomes $\psi = (\phi_f | \phi_\mathcal{H} | \phi_B | \phi_{Bn})$. To render the matrix equation uniquely solvable, we have to add a matrix relation between ϕ_B and ϕ_{Bn} (DtN relation).

---

[1] The *Dirichlet-to-Neumann* relation is the relation between the Dirichlet datum u and the Neumann datum u'

3. The exterior problem

3.1. MATHEMATICAL MODEL

A current moving at velocity U in the positive x-direction is the same as an object moving at speed U in the negative x-direction. We assume the interior to be moving together with the object ('ship-fixed'), while the exterior is fixed to the earth ('earth-fixed') for one time step (see Fig. 2).
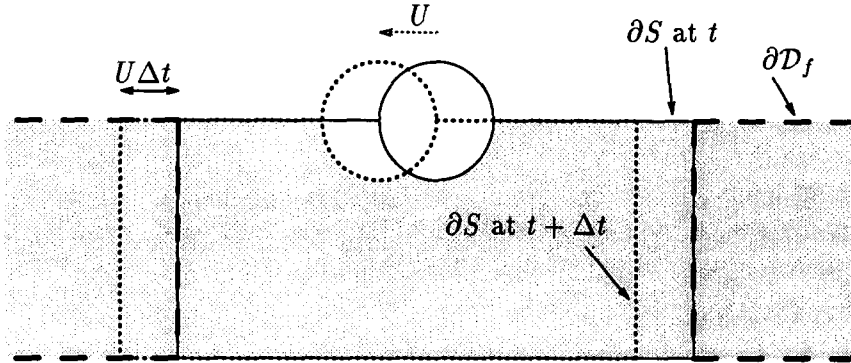

Figure 2. The geometry on t and $t + \Delta t$, earth fixed

In the exterior the velocity potential also has to satisfy the Laplace equation (1) and the bottom condition (4). Because the exterior does not move during a single time step the linearized free-surface condition can be written as follows

$$\phi_{tt} + g\phi_z = 0 \,, \tag{6}$$

where we have neglected ϕ_{dist} in Eq. (3). By making ϕ_z explicit and discretizing ϕ_{tt} by a first-order difference, we get:

$$\phi_{z,i+1} + \frac{1}{g(\Delta t)^2}\phi_{i+1} = \frac{1}{g(\Delta t)^2}\left(2\phi_i - \phi_{i-1}\right) \qquad \text{at } z = 0 \,, \tag{7}$$

with Δt the size of a time step.

3.2. NUMERICAL ALGORITHM

To solve the exterior problem, we introduce a Green's function, G, which satisfies

$$
\begin{aligned}
G_z + \mu G &= 0 & &\text{at } z = 0 \\
\nabla^2 G &= 0 & &x, \xi \in \mathcal{D} \\
G_z &= 0 & &\text{at } z = -h \\
G &= 0; \;\; G_n = 0 & &\lim r \to \infty \,,
\end{aligned}
\tag{8}
$$

with $\mu = 1/(g(\Delta t)^2)$. The last relation is the only physical radiation condition. By using Green's theorem, we get for the potential in the exterior

$$\delta\phi_{i+1}(x) = \int_B \left(\phi_{i+1}(\xi)\frac{\partial G}{\partial n_\xi}(x, \xi) - G(x, \xi)\frac{\partial \phi_{i+1}}{\partial n_\xi}(\xi)\right) dz_\xi$$

$$- \mu \int_{\partial \mathcal{D}_f} G(x, \xi)\left(2\phi_i(\xi) - \phi_{i-1}(\xi)\right) dx_\xi \,, \tag{9}$$

with

$$\delta = \begin{cases} 1 & x \in \mathcal{D} \cup \partial \mathcal{D}_f \\ \frac{1}{2} & x \in \partial \mathcal{B} \\ 0 & \text{elsewhere} \end{cases} ,$$

and $\partial \mathcal{D}_f$ the free surface of the exterior. We need to mention that the normal derivative on the boundary in the exterior is the negative of that of the interior. By analogy with Wehausen et al. [17] we derive a Green's function, which satisfies (8)

$$
\begin{aligned}
G(x, \xi) &= \frac{1}{2\pi} \log r + \frac{1}{2\pi} \log r_2 \\
&\quad - \frac{1}{\pi} \int_0^\infty \frac{e^{-kh}}{k} \left(\frac{(k-\mu)\cosh k(z+h)\cosh k(\zeta+h)\cos k(x-\xi)}{k\sinh kh + \mu\cosh kh} + 1 \right) dk \qquad (10a) \\
&= -\sum_{k=1}^\infty \frac{1}{m_k} \frac{m_k^2 + \mu^2}{hm_k^2 + h\mu^2 + \mu} \cos m_k(z+h)\cos m_k(\zeta+h)e^{-m_k|x-\xi|}, \qquad (10b)
\end{aligned}
$$

with $\boldsymbol{\xi} = (\xi, \zeta)$ and m_k as imaginary parts of the purely imaginary poles.

Wehausen computes the Green's function in the frequency domain, where $\nu = -\mu$ is the wave number ω^2/g, thus the integral equation has a pole at m_0, with $\tanh(m_0 h) = \omega^2/(m_0 g)$. The integral has to be split into a Cauchy principal-value part and a residue. In the time domain the integral equation has no real poles, because $\mu = 1/(g(\Delta t)^2)$. Hence we do not have the residue part. The summation (10b) has been derived by a transformation in the complex plane and by taking the summation of the residues. The imaginary poles in the time domain have to satisfy

$$im_k \tanh(im_k h) = -\mu \qquad \rightarrow \qquad m_k \tan(m_k h) = \mu \qquad m_k \in \mathbb{R} .$$

We have to use the integral form (10a) for small $|x - \boldsymbol{\xi}|$, because the summation (10b) does not converge. This is the reason why the direct DtN approach does not work. By first integrating the Green's function with respect to the surface, the convergence speeds up for both the sum and integral form. Computing the integral form by using the 5-point Gauss-Laquerre quadrature formula is a good approach, but it requires a lot of computer time. A better way is to write the integral as $\int_0^\infty e^{-x} f(x) dx$ and to use fast Gauss-Laquerre integration routines to compute it.

By using Green's theorem we have to integrate the Green's function with respect to ζ or ξ, we are able to write for the potential in the exterior

$$D_\mathcal{D} \psi_B = E_\mathcal{D} \tilde{\phi} , \qquad (11)$$

with ψ_B the vector $(\phi_B | \phi_{Bn})$ and $E_\mathcal{D} \tilde{\phi}$ is the last term of (9).

Upon a more careful reexamination of the paper by Yeung [16], Eq. (9) can be considered as a discrete solution of an 'exact' time-dependent wave-maker solution (Eq. (5.7) in [16]). The 'shell method' is, in essence, of the same form as the DtN relation. Without forward speed, both methods give good results. The advantage of the DtN relation is that we have to compute the Green's function just once. However, the shell method does not need to cover

the free surface of the exterior with panels. To date, there have been no results available from the shell method that include forward speed. It is easier to implement the effects of the double body potential by using the DtN method instead of the shell method. However, by taking into account the double body potential, using the shell method, we also need to define panels at the free surface.

4. Total problem

In the absence of current, at time $t + \Delta t$ the artificial boundary $\mathcal{B}$ of the exterior is the same as the artificial boundary of the interior. Hence, combining Eqs. (5) and (11), we are able to write the interior problem as an overall matrix equation, like Eq. (5),

$$D_1 \psi_{i+1} = D_2 \psi_i + D_3 \psi_{i-1} + f_{i+1} + E_{\mathcal{D}} \tilde{\phi}, \tag{12}$$

with ψ a vector containing $(\phi_f | \phi_{\mathcal{H}} | \phi_{\mathcal{B}} | \phi_{\mathcal{B}_n})$.

If the object is moving with a current U in the negative x-direction, the boundary of the interior moves a distance $U\Delta t$ to the left with regard to the boundary of the exterior. To express the potential on the boundary of the exterior in terms of that of the interior, we apply Green's theorem on the domain between the boundaries (see Fig. 3). Thus we discretize the artificial boundaries and the free surface between the boundaries by dividing these into panels.
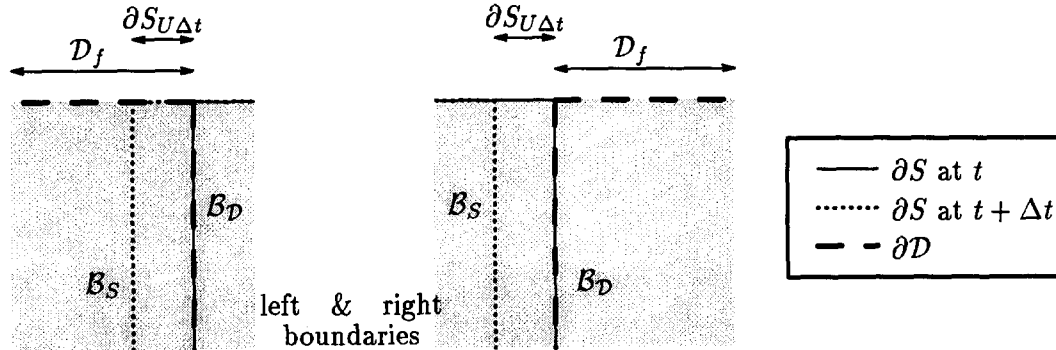

Figure 3. Using Green's theorem at the boundary.

Here we give a derivation for expressing the potential on $\mathcal{B}_{\mathcal{D}}$ in terms of the potential on $\mathcal{B}_S$, in the domain on the left side. The derivation on the right side is analogous, taking proper account of the direction of the normal derivative. By applying Green's theorem in a clockwise direction to the domain between the boundaries, with the normal pointing out of the domain, and using the Green's function which satisfies (8), we get

$$\delta\phi = -\int_{\mathcal{B}_S} \left(\phi \frac{\partial G}{\partial n_\xi} - G \frac{\partial \phi}{\partial n_\xi} \right) d\xi + \mu \int_{\partial S_{U\Delta t}} G\tilde{\phi} \, d\xi + \int_{\mathcal{B}_{\mathcal{D}}} \left(\phi \frac{\partial G}{\partial n_\xi} - G \frac{\partial \phi}{\partial n_\xi} \right) d\zeta, \tag{13}$$

where $\tilde{\phi}$ is the potential on the free surface of the exterior in the past (see Eq. (11)). If we assume ϕ on the boundary $\mathcal{B}_S$, then $\delta = \frac{1}{2}$. By subtracting (9)–(13) we get

$$\frac{1}{2}\phi_{\mathcal{B}_S} = \int_{\mathcal{B}_S} \left(\phi \frac{\partial G}{\partial n_\xi} - G \frac{\partial \phi}{\partial n_\xi} \right) d\zeta + \mu \int_{\partial \mathcal{D}_f \backslash \partial S_{U\Delta t}} G\tilde{\phi} \, d\xi.$$

Now we are also able to define the problem with uniform current speed U as an overall matrix equation such as (12). After computing the potential on the interior and on the artificial boundary, we are able to compute the potential on the free surface of the exterior by using (9). On the right side, the potential $\tilde{\phi}$ on $\partial S_{U \Delta t}$ is defined by the potential on the free surface of the interior and on the left side on that of the exterior.

5. Results

5.1. REFLECTIONS

We first look at the reflections of the artificial boundary, using the algorithm mentioned in the previous sections. We force the cylinder to oscillate harmonically over a time interval of six periods according to the frequency of encounter. During this interval 300 time steps were taken. To have an idea of the reflection, we compare the surface elevation close to the object both when the artificial boundary is far away (so there is no reflection), and when the boundary is close to the object.

Figs. 4 and 5 show the surface elevation versus the horizontal distance from the object. The cylinder is forced to oscillate in heave, there is no current, the depth is infinite and $\omega_0 \sqrt{R/g} = 0.5$. Exactly after a period of oscillation, we plot the surface elevation. It is clear that after a few periods a periodical wave pattern arises next to the object. When there is no reflection (Fig. 4b), after four periods the surface elevation is exactly the same after every following period of oscillation. When there is a total reflection (i.e. a rigid wall at one wavelength, Fig. 5a), the surface elevation changes considerably after every following period. It is also clear that for both the Sommerfeld condition at 3λ and the DtN relation at 1λ the reflection is very small.

We use the wavelength λ defined by

$$\lambda = \frac{2\pi}{k}, \qquad \text{with} \qquad \omega = \omega_0 + kU \qquad \text{and} \qquad k \tan kh = \frac{\omega_0^2}{g},$$
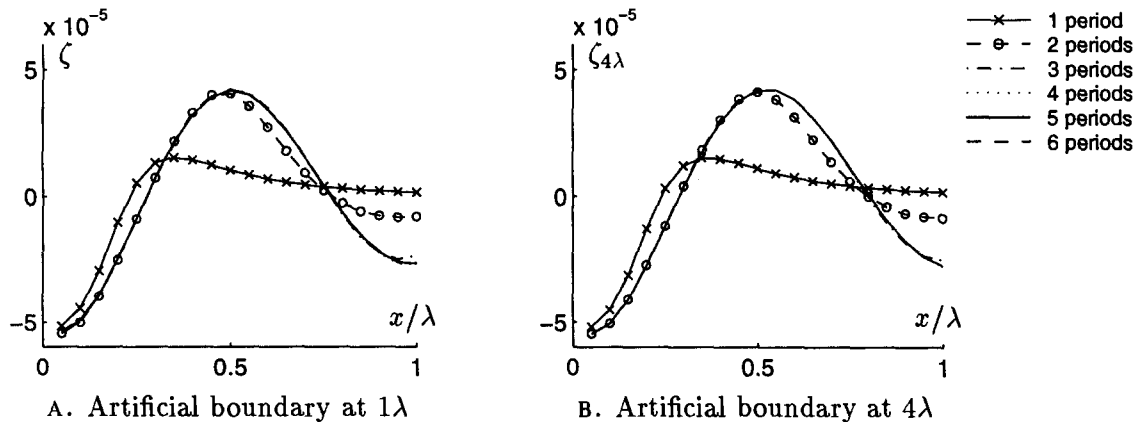
with ω the frequency of encounter.

A. Artificial boundary at 1λ B. Artificial boundary at 4λ

Figure 4. The surface elevation using the DtN method

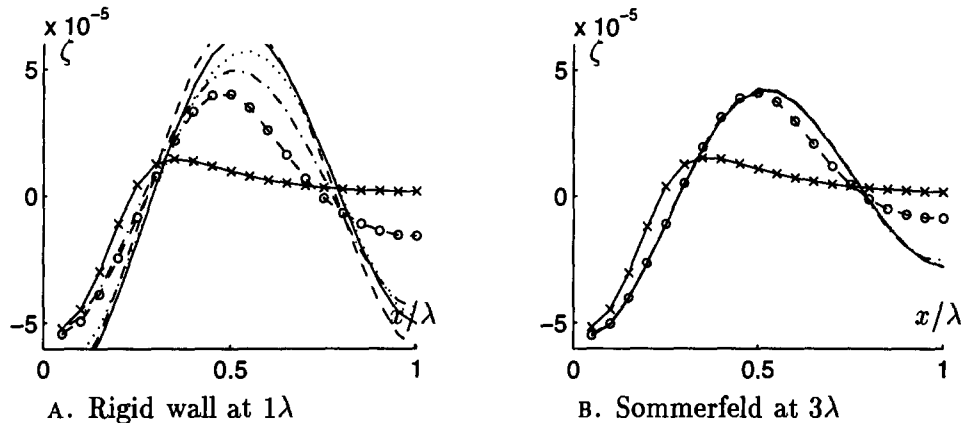A. Rigid wall at 1λ B. Sommerfeld at 3λ

Figure 5. The surface elevation

We studied the case for both infinite depth (i.e. choosing the bottom relatively far away) and the ratio depth/draught equal to 3 (*i.e.* $h/R = 6$). To be able to compare our results with Prins and Hermans's results [4], we look for both $U = 0$, so the Froude number $Fn = U/\sqrt{gR} = 0$, and for $Fn = .14$.

We use about 20 panels on the upstream free surface of the interior and, because of the equidistant grid, more than 20 panels on the downstream free surface. On the artificial boundary and on the free surface of the exterior, the size of an element is twice the size of an element of the interior free surface.

The length of the exterior depends on the length of the time integration. Givoli [8] chooses the length of the exterior such that it is always just ahead of the wave fronts. This length is not constant during time-stepping. We choose the length such that a wave will not be back at the boundary during the time integration. For instance, to compute the added mass and damping we use a time interval of four periods for the frequency of encounter. The length of the exterior is $1\frac{1}{2}$ wavelengths.

In Fig. 6 we show a relative reflection versus the horizontal distance from the object to the boundary for both the Sommerfeld and the DtN relation after 6 periods of forced oscillation. This is also an example with $\omega_0\sqrt{R/g} = 0.5$ and no current. We get the relative reflection by calculating the difference between the surface elevation $\zeta_{4\lambda}$ next to the object when the boundary is far away (no reflections), and when the boundary is closer to the object. This difference is scaled by $\zeta_{4\lambda}$.

To get about the same reflection that Prins gets when using three wavelengths and the Sommerfeld relation, we have to use an interior of about one wavelength. This means that the matrices D_1, D_2, etc. are smaller, so computer time decreases.

Another advantage of our method is that we do not have to update the matrices D_1, D_2, etc. for every wave frequency. This also reduces computer time considerably. We divide the frequency domain such that for one group of frequencies the interior is one wavelength for the smallest ω_0 and two wavelengths for the largest ω_0. There are 30 elements per wavelength for the smallest ω and 15 elements for the largest ω. Using groups, the artificial boundary is more than one wavelength away for all ω, except the smallest, so the reflection will be less if we take the frequencies apart, but we take fewer elements per wavelength, so the computation will be less accurate.
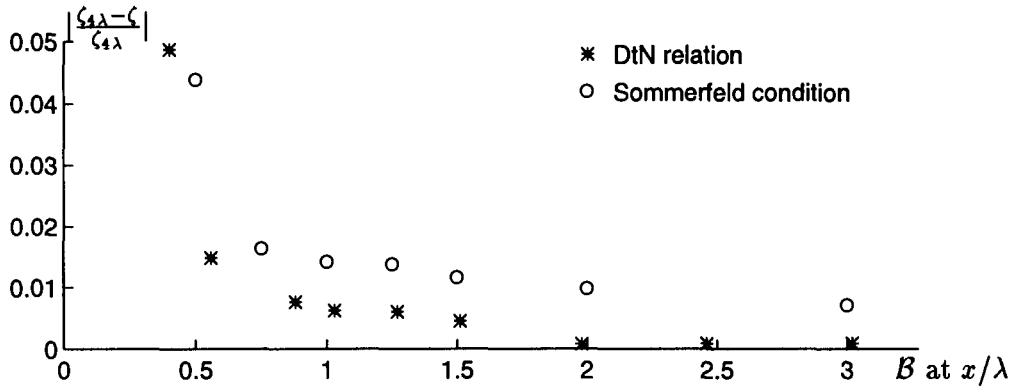
Figure 6. The reflection after 6 periods of forced oscillation.

5.2. THE ADDED MASS AND DAMPING

Knowing the potential due to the diffracted waves, we are able to compute the hydrodynamic coefficients, the added mass and damping matrices A and B, by fitting the first-order forces to the acceleration and the velocity.

$$F = \rho \int_{\mathcal{H}} \left(\frac{\partial \phi}{\partial t} + \nabla \phi \cdot \nabla \overline{\phi} \right) n \mathrm{d}s = -A \frac{\partial^2 X}{\partial t^2} - B \frac{\partial X}{\partial t} \,,$$

with ρ the density of the fluid. Computing the added mass and damping coefficients, (Figs. 7, 8, 9 and 10), is done in groups of frequencies in the same way as mentioned in the previous subsection. This way of computing the coefficients takes much less time than the way in which Prins computes them. For instance, to compute the coefficients in sway at $\omega_0 \sqrt{R/g} = 1$ and $Fn = 0$ we need about 20 sec to fill the matrices and 40 sec to time iterate and compute the coefficients (computations are done on an HP 9000/720 workstation). This is respectively $\frac{2}{3}$ and $\frac{1}{3}$ of the time Prins needed. This is only for one frequency. By using the groups of frequencies we do not have to update the matrices. Thus by using groups of about five frequencies we need only 30% of the time Prins needs to compute them.
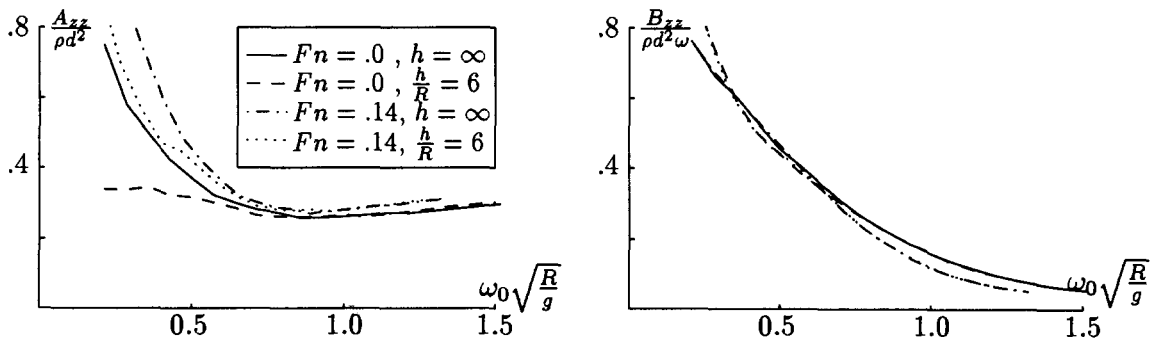

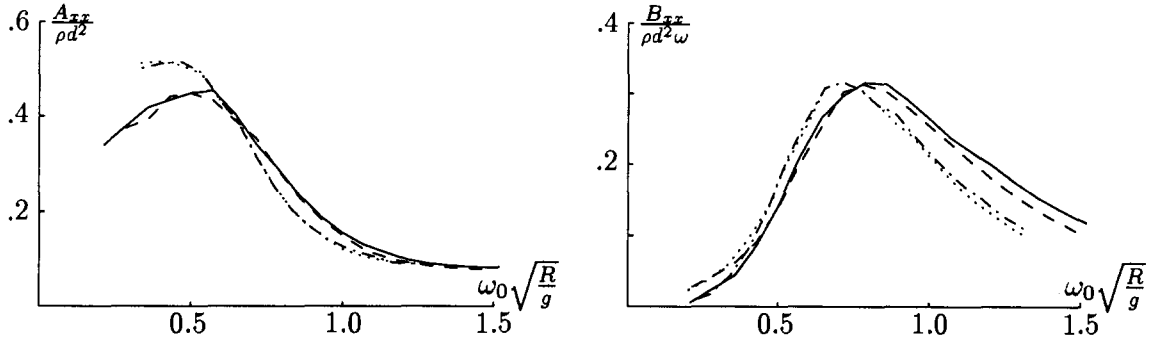*Figure 7.* Added mass and damping in heave.
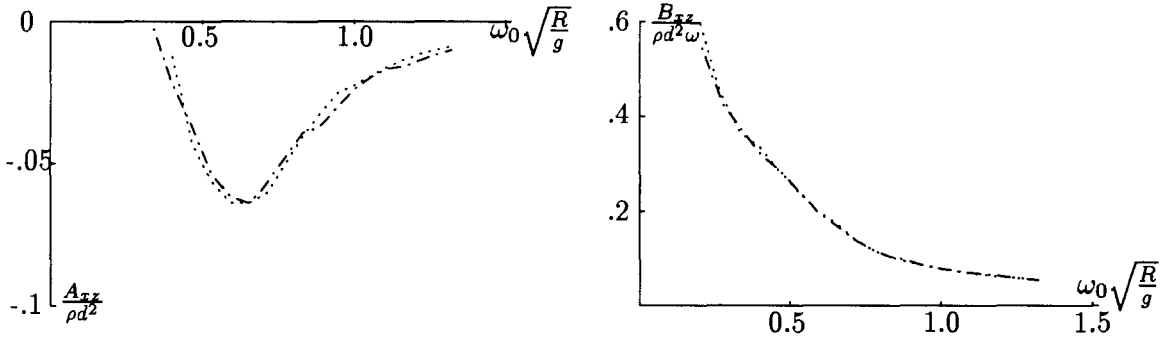
Figure 8. Added mass and damping in sway.

Figure 9. Coupled added mass and damping in heave.

5.3. MOVEMENT AND SECOND-ORDER FORCES

Computing the movement and second-order forces we use as incoming potential in the interior

$$\phi_{inc}(x,t) = \frac{g\zeta_a}{\omega_0} \cos(\omega t - kx)e^{kz} \ ,$$

with ζ_a the wave height due to the incoming wave. The movement X of the ship can then be calculated by solving the following differential equations, with F_1 the first-order forces due to incoming and diffracted waves.

$$F_1 = \rho \int_{\mathcal{H}} \left(\frac{\partial \phi}{\partial t} + \nabla \phi \cdot \nabla \bar{\phi} \right) n ds = (M + A)\frac{\partial^2 X}{\partial t^2} + B\frac{\partial X}{\partial t} + RX \ ,$$
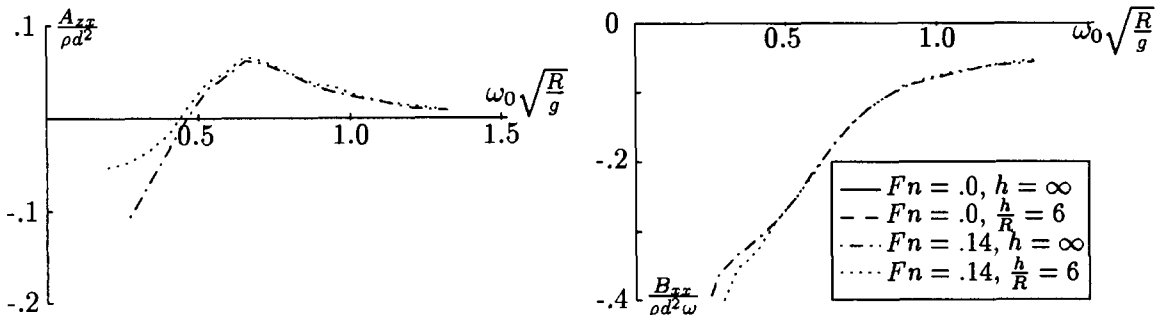

Figure 10. Coupled added mass and damping in sway.

with R the matrix of restoring coefficients, built up by the zero-speed restoring coefficients and the the term $\rho \int_{\mathcal{H}} \nabla\overline{\phi}(X \cdot \nabla)\nabla\overline{\phi}\, n \mathrm{d}s$. After we have calculated the movement of the ship, we are able to compute the potential attributed to this motion. The total unsteady potential is now known, so we can compute the average second order-forces, $\langle F_2 \rangle$, (see Fig. 11), which are correct up to the second order in the velocity, by the following formula:

$$\langle F_2 \rangle = \left\langle -\rho g \left\{ \frac{\zeta_r^2}{2} n \right\}_{x=-R,\, z=0}^{x=R,\, z=0} + \right.$$

$$\left. -\rho \int_{\mathcal{H}} \left\{ (X \cdot \nabla)\left(\frac{\partial\phi}{\partial t} + \nabla\overline{\phi} \cdot \nabla\phi\right) + \frac{1}{2}(X \cdot \nabla)\left(\nabla\overline{\phi}(X \cdot \nabla)\nabla\overline{\phi}\right) + \frac{1}{2}\nabla\phi \cdot \nabla\phi \right\} n \mathrm{d}s \right\rangle ,$$

where ζ_r is the linearized relative wave height.

The time integration was carried out over a time interval of 8 periods according to the frequency of encounter. During this interval 400 time steps were taken. The equations of motion were integrated using Crank-Nicholson's implicit method.
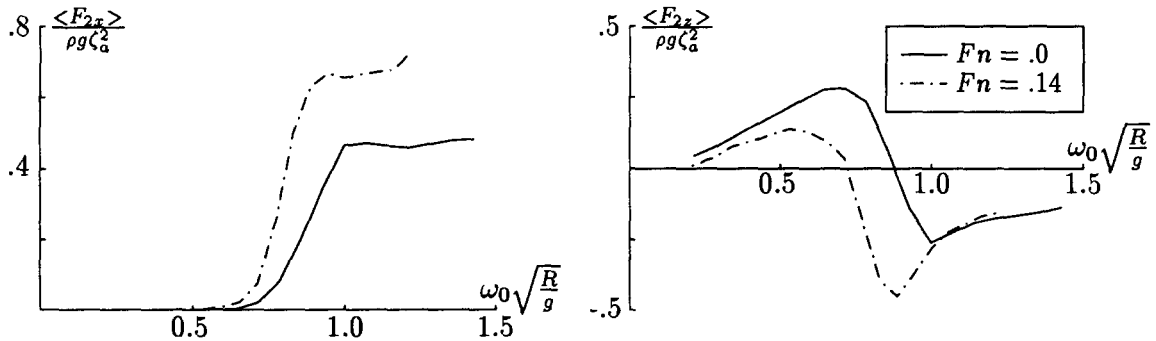

Figure 11. The horizontal and vertical drift force for infinite depth.

6. Conclusions

In this paper we discussed the development of an absorbing boundary condition for floating two-dimensional objects in current and waves, by using time integration. By dividing the physical fluid domain into a computational part and a residual part, we derived a frequency independent numerical algorithm to compute the hydrodynamic coefficients. Computing the special Green's function in the residual part is relatively costly. A faster algorithm will be developed in the future. Our method, however, uses only about one-third of the computer time that was needed when using the Sommerfeld radiation condition at the artificial boundaries. To be able to compare our results with those of Prins and Hermans [4] we only compute the interesting coefficients for a range of frequencies. In the future, we will try to extend the method to general time signals and we will use this method to compute the hydrodynamic coefficients on floating three-dimensional objects in current and waves.

7. Acknowledgements

References

1. R.W. Yeung, The transient heaving motions of floating cylinders. *Journal of engineering mathematics* 16 (1982) 97-119.
2. J.N. Newman, Transient axisymmetric motion of a floating cylinder. *Journal of fluid mechanics* 157 (1985) 17-33.
3. D.E. Nakos, Rankine panel methods for time-domain free-surface flows. *Proceedings of the numerical ship hydrodynamics symposium*, Iowa, USA (1993).
4. H.J. Prins and A.J. Hermans, Time-domain calculations of the drift forces on a floating two-dimensional object in current and waves. *Journal of ship research* 38 (1994) 97-103.
5. H.J. Prins and A.J. Hermans, Time-domain calculations of the second-order drift forces on a floating three-dimensional object in current and waves. *Schiffstechnik* 41 (1994) 85-92.
6. J.E. Romate, *The numerical simulation of nonlinear gravity waves in three dimensions using higher order panel method*. Ph.D. thesis, University of Twente, The Netherlands (1989).
7. J.B. Keller and D. Givoli, Exact non-reflecting boundary conditions. *Journal of computational physics* 82 (1989) 172-192.
8. D. Givoli, *Numerical methods for problems in infinite domains*. Elsevier, Amsterdam, The Netherlands (1992).
9. R. Timman and J.N. Newman, The coupled damping coefficients of a symmetric ship. *Journal of ship research* 5 (1962) 1-7.
10. M. Israeli and S.A. Orszag, Approximation of radiation boundary conditions. *Journal of computational physics* 41 (1981) 115-135.
11. A. Sommerfeld, *Partial differential equations in physics*. Academic Press, New York, USA (1949).
12. I. Orlanski, A simple boundary condition for unbounded hyperbolic flows. *Journal of computational physics* 21 (1976) 251-269.
13. B. Engquist and A. Majda, Absorbing boundary conditions for the numerical simulation of waves. *Mathematics of computation* 31 (1977) 629-651.
14. D.S. Jones and G.A. Kriegsmann, Note on surface radiation conditions. *SIAM Journal of applied mathematics* 50 (1990) 559-568.
15. K.J. Bai and R.W. Yeung, Numerical solutions to free-surface flow problems. *Proceedings of the tenth symposium on naval hydrodynamics*, Cambridge, USA (1974).
16. R.W. Yeung, A comparative evaluation of numerical methods in free-surface hydrodynamics. *Proceedings of the IUTAM symposium on Hydrodynamics of ocean wave-energy*, Lisbon, Portugal (1985).
17. J.V. Wehausen and E.V. Laitone, Surface Waves. *Handbuch der Physik*, Berlin: Springer-Verlag (1960).